EPJ B
Condensed Matter and Complex Systems
EPJ.org
your physics journal

Eur. Phys. J. B (2016) 89: 154 DOI: 10.1140/epjb/e2016-70140-5

A new criterion for melting of nanostructures of arbitrary shapes

Desyana Olenka Margaretta, Mega Silvia Lestari, Bebeh W. Nuryadin and Mikrajuddin Abdullah

edp sciences
Società Italiana di Fisica
Springer

Eur. Phys. J. B (2016) 89: 154
DOI: 10.1140/epjb/e2016-70140-5

THE EUROPEAN PHYSICAL JOURNAL B

Regular Article

A new criterion for melting of nanostructures of arbitrary shapes

Desyana Olenka Margaretta[1], Mega Silvia Lestari[1], Bebeh W. Nuryadin[2], and Mikrajuddin Abdullah[1,a]

[1] Department of Physics Bandung Institute of Technology Jalan Ganeca 10, 40132 Bandung, Indonesia
[2] Sunan Gunung Djati State Islamic University, Jalan A.H. Nasution, Bandung, Indonesia

Received 6 March 2016 / Received in final form 16 April 2016
Published online 20 June 2016 –

Abstract. We introduce a new and general criterion for melting as an alternative to the commonly used Lindemann criterion. Nanostructures are modeled using a zipper model and the melting process is assumed to start from the outer layer and develop towards the center layer. Melting occurs when the logarithm of the partition function per number of layers is zero. The equation shows good consistency with experimental data for the melting of thin films, nanoparticles, and nanowires. We also introduce a degree-of-freedom parameter which seems to be universal for most metals.

1 Introduction

The Lindemann criterion states that melting occurs when the parameter $\xi = \sqrt{\langle \Delta r^2 \rangle}/a$ exceeds the critical value, where $\sqrt{\langle \Delta r^2 \rangle}$ is root mean square fluctuation of atom positions and a is atomic distance [1–4]. Lindemann estimates the parameter ξ around 0.5 [1], although later known to be overestimated. Although the Lindemann criterion is not very accurate (the error can vary between 20%–30%), this criterion is often used as a starting point to derive the melting equation for nanostructures. Comprehensive study on the application of Lindemann criterion to explain the melting phenomenon of nanostructures has been reported by Shi [5], and the basic formulation derived has been used to obtain different forms of equations about the effect of size on the melting point of nanostructures and those equations are still used today [6–13].

We have explained previously that deviations in estimating the Lindemann criterion by 10% may result in deviation in the predicted melting point by 5% [14]. No exact criterion has been proposed to replace the Lindemann criterion. We have proposed a criterion for thin film melting by assumption that melting occurs at the pole of a partition function that has been constructed using a zipper model [14]. Indeed, the zipper model has been discussed by Kittel to describe the transition of molecules [15].

The previous zipper model has been applied only to the thin films [14]. In this paper we will introduce a unique criterion to describe melting of nanostructures with arbitrary shapes. Based on the criterion, we derive a melting equation that can be used for all shapes of nanostructures. We then compare the equation with experimental data for thin films, nanoparticles, and nanowires.

[a] e-mail: mikrajuddin@gmail.com

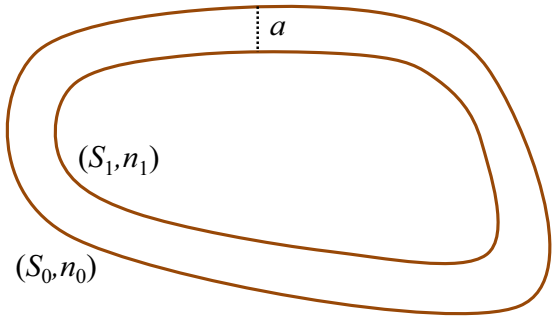

Fig. 1. A nanostructure is divided into layers that have a separation a at each point. The index s moves from the surface ($s = 0$) to the inside.

2 Modeling

Suppose the nanostructure has a surface area S_0 (see Fig. 1). One atom on the surface occupies an area a^2 so that the number of atoms at the surface is $n_0 = S_0/a^2$. Next we create a layer $s = 1$ where each point at the layer has a perpendicular distance a from the surface $s = 0$. We select the index s moves from the surface ($s = 0$) to the inside. The area of this layer is S_1, smaller than S_0. We can write $S_1 = \alpha_1 S_0$ with $0 < \alpha_1 \leq 1$ and the number of atoms in this layer is $n_1 = S_1/a^2$. Then, we create a second layer which has a perpendicular distance a from layer S_1. The area of this layer is $S_2 = \alpha_2 S_0$ with $0 < \alpha_2 \leq 1$ and the number of atoms in this layer is $n_2 = S_2/a^2$, etc.

If the surface $s = 0$ to the layer $s = p$ have already opened then the number of atoms (zipper cells) that is already open is $N_p = \sum_{i=0}^{p} n_i = \frac{S_0}{a^2} \sum_{i=0}^{p} \alpha_i$, with $\alpha_0 = 1$. In this context, the open layer means the melted layer (all atoms in that layer has already transformed from solid

state to liquid state). Because the shape of the material is not always symmetric, the inner layers may be unclosed.

The melting process is assumed to start from the outer layer and develop towards the center layer. The melting process thus starts from the 0th layer. The sth layer melts only if all layers from the 0th layer to the $(s-1)$th layer have melted. If the sth layer has not yet melted then none of the layers from the $(s+1)$th to the center layer can melt. This consideration is likely equivalent to crystal growth process as discussed by Cahn, where the process starts from the outer layer [16]. This is analogous to a zipper mechanism; that is, if a certain cell in the zipper is still closed then none of the subsequent cells can be opened. The zipper model is method for expressing the partition function of a process that develops consecutively to a certain direction.

If ε is energy required to melt one atom or to open one zipper cell (the fusion energy per atom), the energy required to melt layers $s = 0$ to $s = p$ is $E_p = N_p\varepsilon$. We define the total number of layers as n. If one atom has g degrees of freedom and the atoms are uncorrelated each other, the partition function per layer is

$$\frac{Z}{n} = \frac{1}{n}\sum_{p=0}^{n} g^{N_p} e^{-N_p\varepsilon/kT} = \frac{1}{n}\sum_{p=0}^{n} e^{\sigma N_p}, \tag{1}$$

with $\sigma = \ln g - \varepsilon/kT$. It is easy to prove that $n \to \infty$, $\ln(Z/n) \to -\infty$ if $\sigma < 0$, $\ln(Z/n) = \ln(1 + 1/n) \to 0$ if $\sigma = 0$, and $\ln(Z/n) \to +\infty$ if $\sigma > 0$.

Based on definition of σ it is clear that $\sigma < 0$ and $\sigma > 0$ represent low and high temperature states, respectively. It thus becomes very rational to associate $\sigma < 0$ with the solid phase and $\sigma > 0$ with the liquid phase. The special state $\sigma = 0$ represents the melting condition. We can then conclude the melting occurs at temperature that satisfying

$$T_m = \frac{\varepsilon}{k\ln g}. \tag{2}$$

Equation (2) is consistent with the result of Sun et al., where local melting point of nanosolids is proportional to the atomic cohesive energy [17].

Because g is the number of degrees of freedom of an atom in the nanostructure, this parameter should have a relationship with the phonon frequency. We hypothesize that g is proportional to the phonon frequency. Liang et al. have calculated the average phonon frequency as function of nanomaterial sizes [18]. They get theoretical curves that explain a number of experimental data well, such as a Cu thin film and nanocrystal, TiO_2 nanocrystal, Ag thin film and nanocrystal, Si thin film, and Si nanocrystal. Although not proposed explicitly, the function $\omega(r)$ in their report can be approximated by $\omega(r) = \omega_\infty[1 + (r_0/r)^\beta]$, where ω_∞ is the phonon frequency in the bulk state, r is the nanostructure size, and r_0 and β are parameters that depend on the type of material. Theoretical modeling with similar functions of phonon frequency was also reported by Liang et al. [19]. Their model can explain the experimental data of TiO_2 nanoparticles [9,20], Si quantum dots [21], and InP dots [22].

Because we have assumed the degree of freedom is proportional to the average phonon frequency we hypothesize that for nanostructures of arbitrary shapes, g satisfies the following equation

$$g(r) = g_\infty\left[1 + \left(\frac{r_0}{r}\right)^\beta\right] \tag{3}$$

where g_∞ is the number of degrees of freedom in the bulk state, and r_0 is a parameter that states the size of nanostructure. The value r_0 can represent diameter for spherical or cylindrical nanostructures and thickness for thin films. For other shapes of nanostructured, r_0 can be attributed to the radius of gyration.

To determine the fusion energy, we divide the material into a skin with a thickness a and an inner part. The total volume is V and the volume of the skin is aS_0. The effective fusion energy is approximated by

$$\varepsilon_{eff} = \frac{\varepsilon_\infty(V - aS_0) + \varepsilon_s aS_0}{V} = \varepsilon_\infty - (\varepsilon_\infty - \varepsilon_s)a\sigma \tag{4}$$

with $\sigma = S_0/V$ is the specific surface area, ε_∞ is the fusion energy of bulk state (interior atoms) and ε_s is the fusion energy of atoms on the surface. Reduction of the fusion energy of atoms on the surface can be explained by the concept of bond order deficiency [23]. The fusion energy for a single atom is the sum of the single bond energy E_b required to transform a solid state bonding to a liquid state bonding, over all its nearest neighbor (coordinating number), or $\varepsilon = zE_b$ with z is the coordinating number. Atoms on the surface layer is in an under coordinating state so that is has smaller cohesive energy. The under coordinating atoms are only found on the outer layer and less probability to be found on the next layers because all the atoms have neighbor in all directions. Therefore in determining the effective cohesion energy (Eq. (4)), we divided nanostructure only into skin (one layer) and the interior.

Using equations (2), (3) and (4) we get general equation of melting point as a function of the size as:

$$T_m(r) = T_m(\infty)\left\{\frac{1 - \left(\frac{\varepsilon_\infty - \varepsilon_s}{\varepsilon_\infty}\right)a\sigma}{1 + \frac{kT_m(\infty)}{\varepsilon_\infty}\ln\left[1 + \left(\frac{r_0}{r}\right)^\beta\right]}\right\} \tag{5}$$

where $T_m(\infty) = \varepsilon_\infty/k\ln g_\infty$ is the melting point in bulk state.

An important note from equation (5) is that the melting is a collective process that occurs in all atoms forming a material. The effect of size to the melting point does not arise merely as a result of the division of nanostructures on the surface and the interior wherein the surface effect becomes dominant when the size of nanostructures becomes smaller. In equation (5) there is a degree-of-freedom parameter that takes into account the collective contribution of atoms composing the material. Equation (5) states that the melting is caused by two factors: increasing the contribution of surface atoms, which have different cohesion

energy with the interior atoms, and changes in the internal structure when the size of nanostructures becomes smaller as represented by $g(r)$.

Equation (5) is very different from the equations derived by Shi [5] and further discussed by other authors [6–13]. Nearly all equations derived by previous authors satisfy $T_m(r) = T_m(\infty)f(r)$, where $f(r)$ is a function of size only and acts merely as a multiplicative factor [5–13]. The melting point to a different size is just a simple proportionality of melting point in the bulk state. On the contrary, a melting point in equation (5) takes the form $T_m(r) = T_m(\infty)f[r, T_m(\infty)]$, to mean the melting point to a different sizes is not a simple proportionality of the melting point in the bulk state.

Special cases for thin films, nanowires, and spherical particles can be extracted from equation (5). For thin films, $\sigma = 1/r$ where r is the film thickness. For nanowires, $\sigma = \pi Lr/(\pi r^2/4)L = 4/r$ where r is the wire diameter. For spherical particles, $\sigma = \pi r^2/(\pi r^3/6) = 6/r$ where r is the particle diameter. Thus, the size dependent melting points for thin film, nanowire, and spherical nanoparticles can be written as

$$T_m(r) = T_m(\infty)\left\{\frac{1 - D\left(\frac{\varepsilon_\infty - \varepsilon_s}{\varepsilon_\infty}\right)\frac{a}{r}}{1 + \frac{kT_m(\infty)}{\varepsilon_\infty}\ln\left[1 + \left(\frac{r_0}{r}\right)^\beta\right]}\right\} \quad (6)$$

where D is a dimensional parameter, i.e. $D = 1$, 4, and 6, for thin films, nanowires, and spherical nanoparticles, respectively.

3 Comparison with experimental observations

The symbols in Figure 2 are experimental data from the melting of indium thin films grown on Ge substrate [7]. The curve was calculated using equation (6). For comparison we also plot the curves calculated using equation $T_m(r) = T_m(\infty)(1 - \gamma/r)$ [14] and equation $T_m(r) = T_m(\infty)\exp[-(\delta - 1)/(r/2a - 1)]$ [5]. In calculating these curves we used the following parameters: $T_m(\infty) = 429$ K, $\delta = 1.61$ [7] and $a = 0.37$ nm [7] in the last equation, $\gamma = 0.15$ nm in the second equation, and $r_0 = 0.37$ nm [7], $\beta = 1.61$ [7], $D(\varepsilon_\infty - \varepsilon_s)a/\varepsilon_\infty = 0.15$ nm dan $\varepsilon_\infty = 5.40 \times 10^{-20}$ J in equation (6). It is clear that equation (6) can explain the experimental data quite well. In the calculation using equation (6), the parameter r_0 is identical to a in reference [24] and parameter β is identical with δ in reference [24]. Thus, these parameters are not chosen freely, but by using the parameters in references.

Figure 3 is the experimental data for: (a) Pb thin film on a Ge substrate [7], (b) Co particulate thin film co-deposited with SiO_2 [25], (c) nanoparticles Pb [25], (d) nanoparticles Ag [25], (e) In nanowire [26], and Pb nanowire [26]. All curves have been obtained from equation (6) using parameters in Table 1. It is clear that equation (6) is able to fit experimental data very well. In Table 1 almost all parameters are obtained from references [7,14,24,27,28].

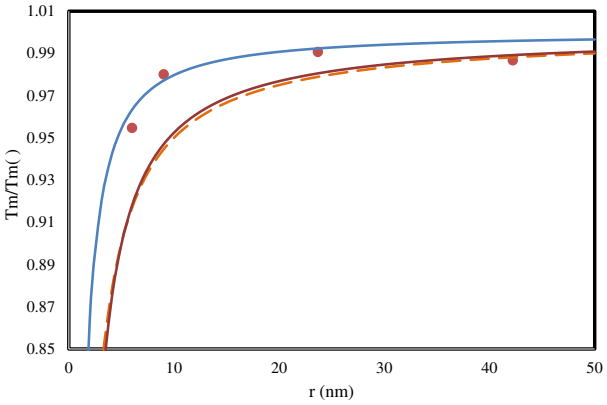

Fig. 2. $T_m(r)/T_m(\infty)$ as a function of film thickness of a thin film of indium on a Ge substrate. Symbols are experimental data [7], the top curve has been obtained from equation (6), the middle curve has been obtained from equation $T_m(r) = T_m(\infty)(1 - \gamma/r)$ [14], and the bottom curve has been obtained from equation $T_m(r) = T_m(\infty)\exp[-(\delta - 1)/(r/2a - 1)]$ [5]. Curve parameters are described in the text.

All figures show a consistency of the model with experimental data. Most nanostructures experience a decrease in melting point with decreasing size. Only Figure 3d, Ag nanoparticles embedded in a matrix of Ni, shows an increase in melting point with decreasing size. In this case, thermal vibration of atoms at the interface are likely to induce superheating [25], leading to a higher melting point.

It is interesting to observe the calculated parameter $g(\infty)$ for various solid groups in the periodic table. Figure 4 gives the parameter $g(\infty)$ as a function of melting point in the groups (a) IA and IIA, (b) transition metals, (c) lanthanides, and (d) IIIA-VIA [8]. Except for the IIIA-VIA groups, the values of $g(\infty)$ seem to be universally about 2–3. The IIA-VIA groups showed more scattered $g(\infty)$ values, and greater than the values owned solids from other groups. This is probably because the atoms in this group are united by covalent bonds, while in the other groups the atoms are joined by metal or ionic bonds.

4 Conclusion

In conclusion, a new criteria for melting has generated a new equation for melting of all shapes of nanostructures. The equation shows good consistency with experimental data for the melting of thin films, nanoparticles, and nanowires. The introduction of a parameter for the degree of freedom is nearly universal for most metals.

Author contribution statement

D.O.M. and M.S.L contributed in processing the data and comparing the experimental and theoretical model. B.W.N and M.A derived the theoretical model. D.O.M contributed partly in writing manuscript draft and M.A. completely wrote the manuscript.

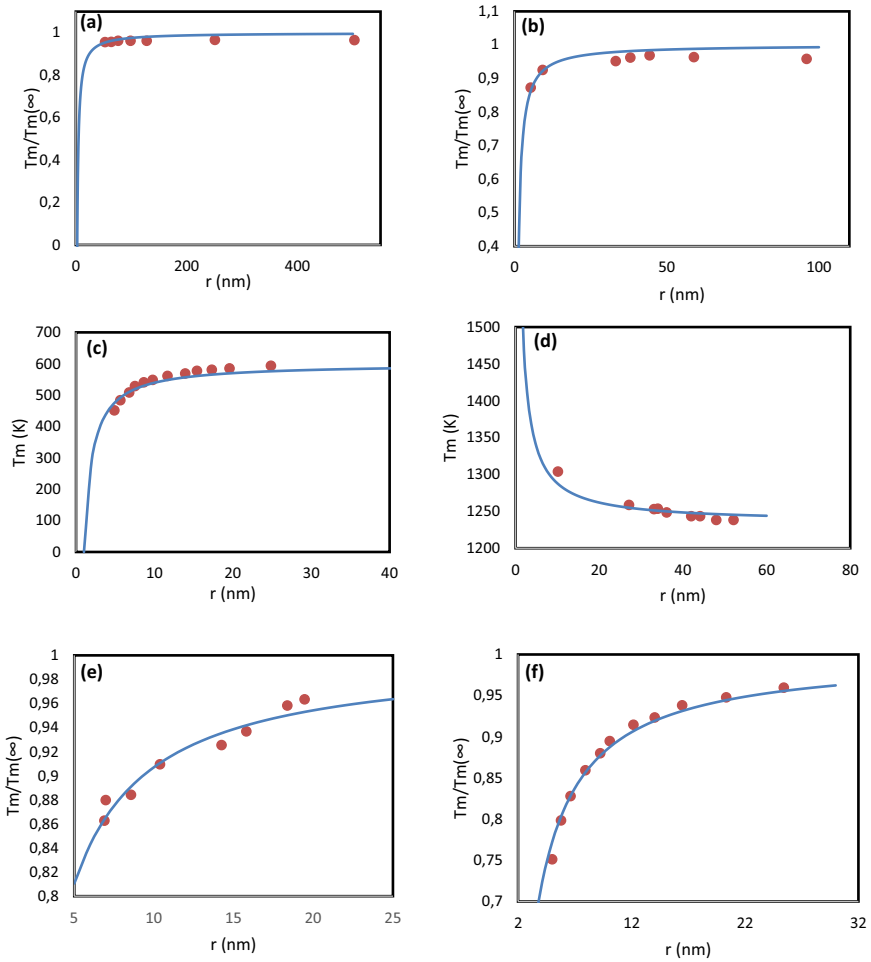

Fig. 3. The experimental data on the melting points of several nanostructures and curves calculated using equation (6). (a) Pb thin film on a Ge substrate [7], (b) Co particulate thin film co-deposited with SiO_2 [25], (c) nanoparticles Pb [25], (d) nanoparticles Ag [25], (e) In nanowire [26], and Pb nanowire [26]. The fitting parameters are listed Table 1.

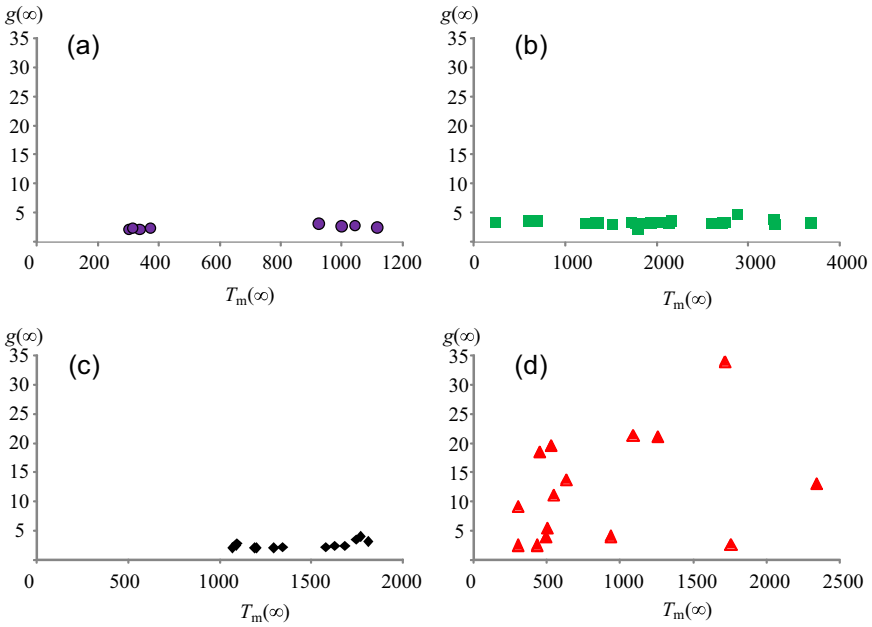

Fig. 4. Parameter $g(\infty)$ as a function of melting point in the groups of (a) IA and IIA groups, (b) transition metals, (c) lanthanides, and (d) IIIA-VIA groups [14].

Table 1. The parameters applied to equation (6) for calculating the curves in Figure 3.

Chart	$T_m(\infty)$ [K]	$D(\varepsilon_\infty - \varepsilon_s)a/\varepsilon_\infty$ [nm]	r_0 [nm]	β	ε_∞ [$\times 10^{-20}$ J]
(a)	600	2.4	0.39 [7]	1.66 [7]	2.29 [14]
(b)	505	0.7	0.62 [7]	2.11 [7]	1.16 [14]
(c)	600	1.0	0.39 [7]	1.66 [7]	2.29 [14]
(d)	1234	–0.45	0.28 [27]	1.73 [28]	1.88 [14]
(e)	429	0.73	0.37 [24]	1.61 [24]	5.40 [14]
(f)	600	1.12	0.39 [7]	1.66 [7]	2.29 [14]

This work was supported by a research grant (No. 310y/I1.C01/PL/2015) from the Ministry of Research and Higher Education, Republic of Indonesia.

References

1. F.A. Lindemann, Physik. Z. **11**, 609 (1910)
2. J.J. Gilfarry, Phys. Rev. **102**, 308 (1956)
3. A.C. Lawson, Philos. Mag. B **81**, 255 (2001)
4. M. Roos, Phys. Rev. **184**, 233 (1969)
5. F.G. Shi, J. Mater. Res. **9**, 1307 (1994)
6. Q. Jiang, N. Aya, F.G. Shi, Appl. Phys. A **62**, 627 (1997)
7. Q. Jiang, H.Y. Tong, D.T. Hsu, K. Okuyama, F.G. Shi, Thin Solid Films **312**, 357 (1998)
8. Y.F. Zhu, J.S. Lian, Q. Jiang, J. Phys. Chem. C **113**, 16896 (2009)
9. W.F. Zhang, Y.L. He, M.S. Zhang, Z. Yin, Q. Chen, J. Phys. D **33**, 912 (2000)
10. Q. Jiang, S. Zhang, M. Zhao, Mater. Chem. Phys. **82**, 225 (2003)
11. Q. Jiang, F.G. Shi, Mater. Lett. **37**, 79 (1998)
12. Z. Zhang, X.X. Lu, Q. Jiang, Physica B **270**, 249 (1999)
13. Z. Liu, X. Sui, K. Kang, S. Qin, J. Phys. Chem. C **119**, 11929 (2015)
14. M. Abdullah, S. Khairunnisa, F. Akbar, Eur. J. Phys. **37**, 015501 (2016)
15. C. Kittel, Am. J. Phys. **37**, 917 (1969)
16. J.W. Cahn, Acta Met. **8**, 554 (1960)
17. C.Q. Sun, Y. Wang, B.K. Tay, S. Li, H. Huang, Y.B. Zhang, J. Phys. Chem. B **106**, 10701 (2002)
18. L.-H. Liang, H. Ma, Y. Wei, J. Nanomater. **2011**, 670857 (2011)
19. L.-H. Liang, C.-M. Shen, X.-P. Chen, W.-M. Lau, H.-J. Gao, J. Phys: Condens. Matter **16**, 267 (2004)
20. D. Bersani, P.P. Lotici, X.Z. Ding, Appl. Phys. Lett. **72**, 73 (1998)
21. X.H. Hu, J. Zi, J. Phys: Condens. Matter **14**, L671 (2002)
22. M.J. Seong, O.I. Micic, A.J. Nozik, A. Mascarenhas, Appl. Phys. Lett. **82**, 185 (2003)
23. C.Q. Sun, Prog. Solid State Chem. **35**, 1 (2007)
24. Z. Zhang, J.C. Li, Q. Jiang, J. Phys. D **33**, 2653 (2000)
25. S. Xiong, W. Qi, Y. Cheng, B. Huang, M. Wang, Y. Li, Phys. Chem. Chem. Phys. **13**, 10652 (2011)
26. A. Safaei, M.A. Shandiz, S. Sanjabi, Z.H. Barber, J. Phys.: Condens. Matter **19**, 216216 (2007)
27. W. Luo, W. Hu, S. Xiao, J. Phys. Chem. **112**, 2359 (2008)
28. C.C. Yang, Y.-W. Mai, Mater. Sci. Eng. R **79**, 1 (2014)